DESIGN AND DEVELOPMENT OF A LOW PRESSURE TURBINE FOR TURBOCOMPOUNDING APPLICATIONS

Aman M.I. Mamat, Alessandro Romagnoli[1] and Ricardo F. Martinez-Botas[2]

[1]Department of Mechanical Engineering
Imperial College of Science, Technology and Medicine
Exhibition Road, London SW7 2AZ, UNITED KINGDOM
[2]Phone: +44 (0)20 7594 7241, Email: r.botas@imperial.ac.uk

ABSTRACT

This paper describes the development of a high performance low pressure turbine (LPT) for turbocompounding applications to be used in a 1.0 litre "cost-effective, ultra-efficient gasoline engine for a small and large segment passenger car". Under this assumption, a mixed-flow turbine was designed to recover latent energy of discharged exhaust gases at low pressure ratios (1.05 - 1.3) and to drive a small electric generator with a maximum power output of 1.0 kW. The design operating conditions were fixed at 50,000 rpm with a pressure ratio of 1.1. Commercially available turbines are not suitable for this purpose due to the very low efficiencies experienced when operating in these pressure ratio ranges.

The low pressure turbine performance was simulated using a commercial CFD software. Then, turbine performance was validated with a comprehensive turbine testing that was accomplished by using the Imperial College turbine test rig. The testing and the simulation conditions were conducted for a range of design equivalent speeds spanning between 80% and 120% at steps of 10% increase.

In addition, the impact of the turbocompounding on Brake Specific Fuel Consumption (BSFC) and Brake Mean Effective Pressure (BMEP) was also assessed by using a 1-D validated engine model of the engine under study. Three different arrangements for the turbocompounding were assessed: (1) pre-catalyst, (2) post-catalyst and (3) in the wastegate of the main turbocharger. The outcomes of the simulation were compared to those obtained for the baseline engine and are discussed in the the paper. The 1-D engine simulation had shown that the maximum benefit of the turbocompounding can be achieved when it was located at the post catalyst with maximum BSFC reduction of 2.4% at 1500 rpm and 3.0% of BMEP increase at 1000rpm.

Keywords: Turbine, Engine downsizing, Turbocompounding, Energy Recovery

NOMENCLEATURE

BMEP	Brake Mean Effective Pressure	[bar]
BSFC	Brake Specific Fuel Consumption	[kg/kW/hr]
C	Absolute Flow Velocity	[m/s]
CCP	Combined Cycle Power	
d	Diameter	[m]
GHG	Greenhouse Gas	
ICE	Internal Combustion Engine	
k	Specific Heat Ratio	
$\dot{m}$	Mass Flow Rate	[kg/s]
MFP	Mass Flow Parameter	$\left[\frac{\text{kg}}{\text{s}}\frac{\text{K}^{0.5}}{\text{Pa}}\right]$
ORP	Organic Rankine Cycle	
P	Pressure	[Pa]
PR	Pressure ratio	
R	Gas Constant	[kJ/kg.K]
T	Temperature	[K]
U	Rotor Velocity	[m/s]
VR	Velocity Ratio	
WHR	Waste Heat Recovery	
η	Efficiency	

Subscript

0	Total/Stagnation Condition
1	Volute Inlet
2	Stator Inlet
3	Rotor Inlet
4	Rotor Exit
is	Isentropic
t-s	Total-to-static

BACKGROUND AND OBJECTIVES

Most heat engines convert only about 20% to 50% of the supplied energy into mechanical work whereas the remaining energy is lost. Although some of the energy lost is intrinsic to the nature of an engine and cannot be fully overcome (such as energy lost due to friction of moving parts), a large amount of energy can potentially be recovered. The current paper will focus on an energy recovery systems for exhaust gases. Besides being important to improve engine performance, the recovery of energy from the exhaust gases is likely to be needed to meet future emission legislations.

The automotive industry aggressively looking into new methods to reduce CO_2 emissions, the current trend is that of using highly boosted downsized engines including a turbocharger and/or a supercharger. This has a significant impact in improving engine performance with a reduction in *BSFC* and hence in CO_2 emissions.

The turbocharger/supercharger boosting system for engine downsizing is a double stage compression option that may include an electrically driven compressor. The electrically driven compressor is known as *electric booster* and it is usually powered by an additional battery element. Due to the presence of the electric booster, it would be advantageous to have an electric generator to meet its higher power electrical demand. At this purpose, a small turbine positioned downstream of the main turbocharger could be used to run this generator. Such an arrangement is known as *electric turbocompounding*.

As part of a TSB[1] project called HyBoost, the current study focuses in the design and the development of a low pressure

[1] The Technology Strategy Board is an executive non-departmental public body (NDPB), established by the Government in 2007 and sponsored by the Department for Business, Innovation and Skills (BIS).

Presented at International Gas Turbine Congress 2011 Osaka, November 13-18, Osaka, Japan, IGTC2011-0052
Review completed July 31, 2012

turbine for turbocompounding applications. The operational constraints for electric turbocompounding systems are mainly due to the electric machine which needs to run at an optimum speed over the entire engine driving cycle in order to work efficiently. In the heavily downsized engine such a requirement is particularly difficult to be achieved since at low engine rpm (below 1500 rpm), the low pressure ratio available (1.05-1.3) constraints the turbine to operate in a region where conventional turbines provide less than 40% efficiency. Figure 1 shows the current limitations where it is a given an example of the efficiency of a medium capacity turbine rotor designed to operate at 98,000 rpm and PR of 1.6. The figure shows the region of interest for turbocompounding superimposed to a conventional turbine map. It is apparent that in a low pressure ratio region a conventional turbine results in really poor turbine efficiency. This paper shows the design and development of a low pressure turbine for turbocompounding applications and its impact on the overall engine performance.

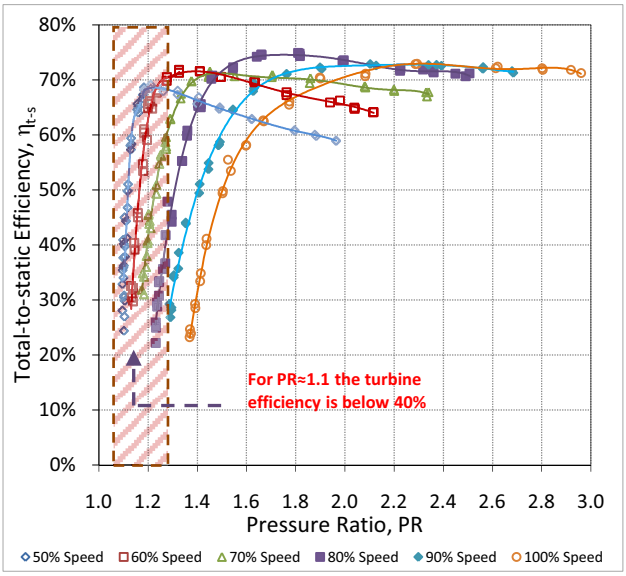

Figure 1: Mixed-flow turbine performance

LITERATURE REVIEW

Internal Combustion Engine (ICE) is the prime mover for transportation. There are four key challenges in the ICE for the energy context, which are; (i) enforce strict emissions legislation and control, (ii) use sustainable new fuels, (iii) reduce fuel consumption and (iv) enhance energy saving concepts [1]. Authorities are using several strategies such as taxation scheme on CO2 emission based and consequently the industries are applying engine downsizing, variable compression ratios, alternative fuels from sustainable sources and advance fuel injection system in order to achieve these key challenges and improve the ICE efficiency. Despite the improvement of the efficiency, the nature of ICE is producing about 25% to 35% of the wasted energy through exhaust gases. Therefore, it is apparent the need to implement advanced concept systems to recycle the wasted energy. At the present, three exhaust energy recovery techniques can be identified:

1. Rankine bottoming cycle
2. Thermoelectric generator
3. Turbocompounding

Srinivasan et al. [2] combined an Organic Rankine Cycle (ORC) to an ICE to recover exhaust gas energy. The available temperature to be recovered in the ICE exhaust varies between 500K to 1000K. A Waste Heat Recovery (WHR) evaporator, that was located after the turbocharger, was used to transfer this exhaust temperature energy from the ICE to the ORC. Then, the high pressure ORC working fluid had changed its phase from a compressed liquid to a superheated vapour. Thereafter, the working fluid was expanded in the turbine and produced 2 kW power. It must be noticed that the energy recovery method explained in ref [2-8] were applied to a dual circuit working fluid that extracted the wasted energy in the upper cycle by using the heat exchanger (Rankine bottoming cycle). Thus the efficiency of the energy recovery depends on the heat exchanger effectiveness. Moreover, the recovery system from ORC is space consuming and not easy to assemble. Therefore, the closed circuit combined cycle is not a favourable solution for a micro heat engine that is used for small scale applications such as domestic air conditioning and automotive power train. Consequently, a high performance and compact devices that is easily attached to the heat engine is usually preferred.

Thermoelectric generator is another exhaust energy recovery technique that can be used and easily attached to the ICE. The principle behind the thermoelectric generator is that of converting the thermal energy of the exhaust gases into electric energy by relying on the Peltier-Seebeck effect. The electric current is produced from a temperature difference between each surfaces of the thermoelectric generator and the exhaust pipe. The temperature difference causes the charge carriers in the thermoelectric material to diffuse from the hot side (exhaust pipe) to the cold side (thermoelectric surface) and this is known as thermally induced current. The implementation of thermoelectric on the ICE is expected to improve its fuel consumption by 10% without increasing emissions [9]. Despite the lightweight nature of thermoelectric devices and the variety of application such as solid-state cooling, heating and power generation, the efficiency of electric conversion is still poor and requires a large surface area for the device. Moreover, the material cost for the thermoelectric generator is still expensive. Thus, further development to improve its energy conversion is required prior its commercialization.

Another method to recover exhaust energy from ICE is that of using a tubocompounding. This method is easier to assemble than the Rankine's bottoming cycle and cheaper than the thermoelectric device solution. The electrical turbocompounding can be easily bolt-on as part of the ICE assembly and can directly be coupled to either the shaft of the main turbocharger or attached to a secondary turbine positioned downstream the main turbocharger [10-14]. If the second options is going to be adopted, as one can expect the energy available in the exhaust gases is not large since most of the expansion occurs in the HP turbine and hence the second turbine has to be operated at lower pressure conditions. For instance in a small car segment the mass flow rate of the exhaust gases is in the range of 0.02 kg/s to 0.1 kg/s and the available pressure at the exit of the main turbine is about 1.1 to 1.3 bar. At such low rate of pressure and mass flow, commercially available turbines fail to provide an adequate response thus justifying the need for a high performance low pressure turbine design.

LOW PRESSURE TURBINE DESIGN

In this section a description of the design procedure followed to develop the low pressure turbine under study is presented. For reasons of space, only a general overview of the entire process is provided here but, for an extensive and more detailed analysis, the reader can refer to previously published work by the authors [15].

Table 1: Turbine Operating Requirement

Turbine Power	1 kW
Turbine expansion ratio	1.1
Blade rotational speed	50000 rpm
Total inlet temperature	1100 K

The operating conditions which were taken as reference for the turbine design are given in Table 1. The turbine design started with a non-dimensional mean-line loss model to define its 2-D rotor features. Mean-line modelling is a simple and reliable tool which is widely used by numerous researchers for preliminary design before fixing the blade geometry [16-18]. After the mean-line model analysis was completed, an assessment on the best turbine geometry was carried out (either radial or mixed-flow).

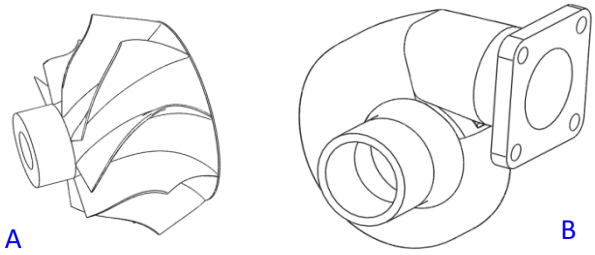

Figure 2: Low pressure turbine, 3-D view of the turbine wheel (A) and volute (B)

Despite the many advantages of radial turbines, they have less geometrical flexibility due to the zero blade angle limitation which makes it difficult to achieve the optimum incidence angle [19-22]. On the contrary a mixed-flow turbine is a naturally back-swept wheel that offers two additional degrees of freedom, such as cone angle, γ and blade angle, β_{bl} [20] while still maintaining its structural stability [21]. This results in a greater flow capacity and in a reduction of the flow path curvature which effectively reduces the formation of secondary flow. This is one of the main advantages of a mixed-flow turbine in respect to the radial counterpart [23] and one of the reasons why it was decided to develop the low pressure turbine as a mixed-flow turbine. After set up the main geometric features of the newly designed turbine, an exhaustive 3-D and CFD analysis was carried out [15] by using a 3-D Solidwork and Ansys CFX, respectively. The final outcome of the turbine design is shown in Figure 2.

Table 2: Low pressure turbine geometric specifications and comparison with commercial turbines

			Low pressure turbine	
Number of Blades, Z			9	
Leading Edge Root Mean Square Radius, $r_{3,rms}$			42.2 mm	
Trailing Edge Tip Radius, d_4			22.7 mm	
Cone angle, γ			20°	
Inlet Blade Angle, β_{bl}			varied	
Rotor blade length, l			33.5 mm	
			Comparative study	
	A_4/A_3	$\eta_{t\text{-}s,design}$	Speed[rpm]	PR
Low pressure turbine (LPT)	0.35	>70%	50000	1.1
Turbine A - High capacity	1.1	80%	60000	2.0
Turbine B -Medium capacity	0.9	84%	98000	1.6
Turbine C- Small capacity	0.8	72%	160000	2.0

The geometric specifications of the newly designed turbine are provided in Table 2 which also provides a comparative study between commercially available turbines and their design values. From the table, it is apparent that the design point for the low pressure turbine is out of the conventional turbines range and this corresponds to a very low area ratio value (A_4/A_3) when compared to standard turbocharger turbines. Such a low value for the area ratio is rather unique and such a constraint was one of the main challenges which had to be solved during the design process.

Finally a prototype for the low pressure turbine was made and installed in the Imperial College test rig as shown in Figure 3. The turbine wheel was made out of Aluminium Al-6082 with 1.6μm surface finish. The turbine volute and the connecting duct instead were made out of polycarbonates (PC) material and manufactured by using a 3-D Fused Deposition Modelling (FDM) machine. The application of polycarbonates for cold-flow testing turbine volute is a novel technique in the turbomachinery research. The main advantages are associated with reduced design lead time and cheaper than a die-cast metal model.

Figure 3: LPT installed in the Imperial College cold-flow test facility

EXPERIMENTAL SET UP

The final step for the design of the low pressure turbine was testing in the cold-flow test facility available at Imperial College. This is a state-of-the-art test facility which enables to obtain turbine maps three/four times wider (with respect to pressure ratio) than those which can be obtained using a compressor as a loading device. Such a large width of the maps can be obtained thanks a bespoke eddy-current dynamometer which loads the turbine through a magnetic rotor coupled to the turbine wheel thus overcoming the limitation of choking and surge typical of a compressor device [24; 25]. Although extensively explained in previously published works by the Imperial College Turbocharger Research Group[2], it is worth it briefly going through the main features of the test facility.

The layout and main components of the test facility are illustrated in Figure 4. The test-rig is supplied by three Ingersoll Rand screw-type compressors, capable to deliver up to 1 kg/s compressed air at maximum pressure of 5 bars (absolute). The air is filtered through a three-stage cyclone and paper filter system. Downstream of the filter system, there is a motorised valve, computer controlled from outside the test-cell for regulating the mass flow rate of air into the turbine. The heaters are regulated by West 4200 PID controller linked to a local thermocouple, where the user-specified flow temperature (300K – 315K) is maintained throughout the testing period. Downstream of the heater stacks, the airflow is branched into two pipes which are called 'inner' and 'outer' limb, referring to its relative position as shown in Figure 4. The two separated streams of airflow from each limb passes through a rotary air pulse generator, which

[2] Imperial College Turbocharger Research Group website: www.imperial.ac.uk/turbochargers

consists of two rotating chopper plates replicating the pressure profiles of an ICE (for unsteady flow testing). In the current study only steady state testing were conducted and therefore the chopper plates were locked in open position. Downstream of the pulse generator, the warm airflow is monitored through an instrumented test-section, called the 'measurement plane', which is instrumented with static pressure tapping and thermocouples in both the inner and outer limb. After the 'measurement plane' the warm airflow finally goes through the connecting duct and into the turbine stage. The turbine is coupled to the eddy current dynamometer with maximum power absorption of 60 kW. The dynamometer is instrumented with a low capacity single point 600 g load cell for the direct torque measurement and an optical speed sensor for the speed measurement.

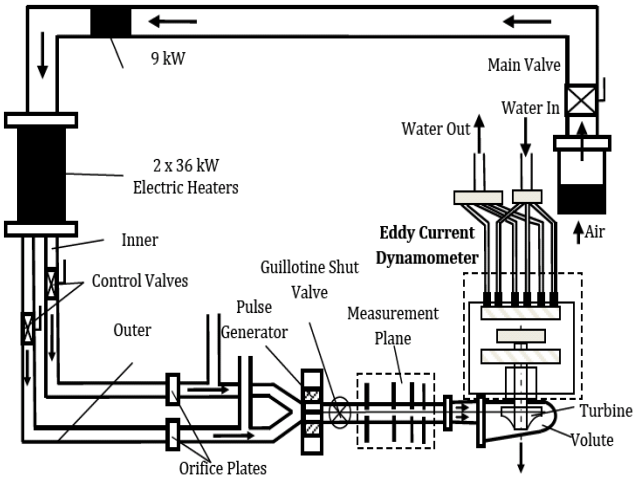

Figure 4: Imperial College cold-flow test facility

PERFORMANCE PARAMETERS

The basic parameters which influence the behaviour of a turbocharger turbine can be grouped in a functional relation as:

$$f(d_3, N, \dot{m}, P_{01}, P_4, T_{01}, T_4, R, k, \mu) = 0 \quad (1)$$

Subscript 1 and 4 refer to volute inlet and rotor outlet respectively. Subscript 2 refers to stator inlet and subscript 3 refers to rotor inlet. By rearranging the terms of Eq. (1), the performance parameter characteristics reduce to six non-dimensional groups:

$$f\left(\frac{P_{01}}{P_4}, \frac{T_{01}}{T_4}, \frac{\dot{m}\sqrt{RT_{01}}}{P_{01}d_3^2}, \frac{Nd_3}{\sqrt{RT_{01}}}, \frac{\dot{m}}{\mu d_3}, k\right) = 0 \quad (2)$$

Commonly the characteristic dimension, d_3 the gas constant, R, and the specific heat ratio, k are dropped from the non-dimensional parameters as they remain constant for a given flow and geometry. Eq. (2) thus simplifies into four main parameters which are given in Eq. (3).

$$f\left(\frac{P_{01}}{P_4}, \frac{\dot{m}\sqrt{T_{01}}}{P_{01}}, \eta_{t-s}, \frac{U_3}{C_{is}}\right) \quad (3)$$

where P_{01}/P_4 is the total-to-static pressure ratio, PR of the whole turbine stage, $\frac{\dot{m}\sqrt{T_{01}}}{P_{01}}$ is the pseudo non-dimensional mass flow rate (defined as Mass Flow Parameter, MFP), η_{t-s} is the total-to-static efficiency and U_3/C_{is} is the velocity ratio, VR. The total-to-static efficiency, η_{t-s} is defined as the as the ratio between the actual power and the isentropic power of the turbine whereas the velocity ratio, VR is a dimensionless parameter defined as the ratio between the rotor tip speed,U_3 and the isentropic or spouting velocity, C_{is}.

The Mass Flow Parameter, MFP is usually plotted against the pressure ratio, PR whereas the efficiency, η_{t-s} is plotted against the velocity ratio, VR.

TURBINE PERFORMANCE

The performance of the newly designed turbine was tested for a set of five different constant speed lines spanning from 80% to 120% equivalent speed lines corresponding to 40,000 rpm and 60,000 rpm of the actual rotational speed. The performance parameters as described in the previous section (MFP, PR, η_{t-s} and VR) were acquired and normalised against the turbine design values[3]. The outcomes of the experimental results are reported in Figures 5 to 8.

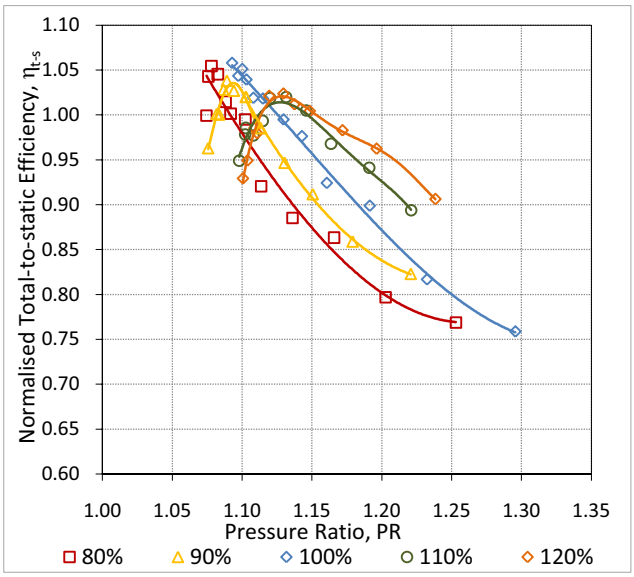

Figure 5: Normalised η_{t-s} vs. PR for cold-flow test

Figure 5 and 6 show the η_{t-s} plotted against the pressure ratio, PR and the velocity ratio, VR respectively. Figure 5 clearly shows that turbine operates at very low pressure ratios - 1.07 to 1.3 - for which the maximum turbine efficiency was measured. For the range of speeds tested all the efficiencies fall between 0.75 to 1.07 of normalised η_{t-s} and this demonstrates the excellent performance of the newly designed turbine in the specified pressure ratio range. Although the magnitude of the optimum efficiency is clearly important, the location where it occurs is also significant to the designer. The location of peak efficiency should correspond to the predominant operating condition of the turbine for the particular engine applications.

Figure 6 shows the relationship between the η_{t-s} of the turbine and the velocity ratio under which it is operating. The velocity ratio correlates the speed of the rotor to its driving fluid. Thus, the curve produces a curve with a maximum value as this is the condition where the fluid flow is best matched to the spinning rotor. For a radial turbine, the peak efficiency occurs at the value of ≈0.7 velocity ratio whereas for mixed-flow turbine it occurs at a lower value. From Figure 6, it can be noticed that peak efficiency point for the low pressure turbine occurs at ≈0.68 for 100% speed. This is fully consistent with the features and

[3] For the efficiency the design value of the total-to-static efficiency is greater than 70%.

requirements of a mixed-flow turbine and it is a sign of the effectiveness of the design procedure followed.

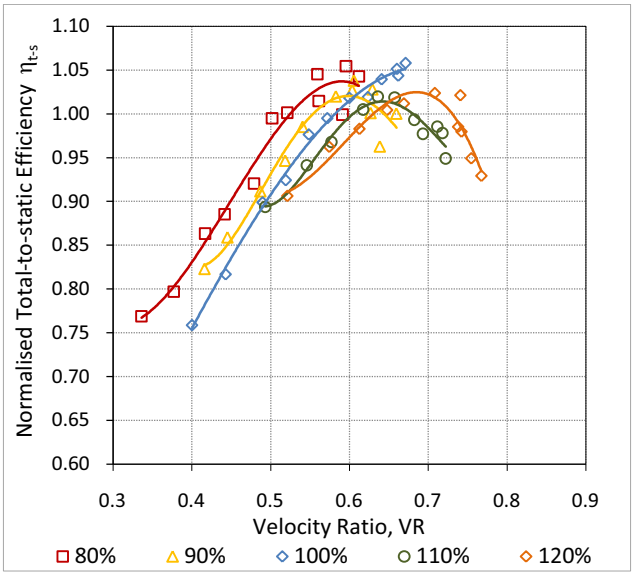

Figure 6: Normalised $\eta_{t\text{-}s}$ vs. VR for cold-flow test

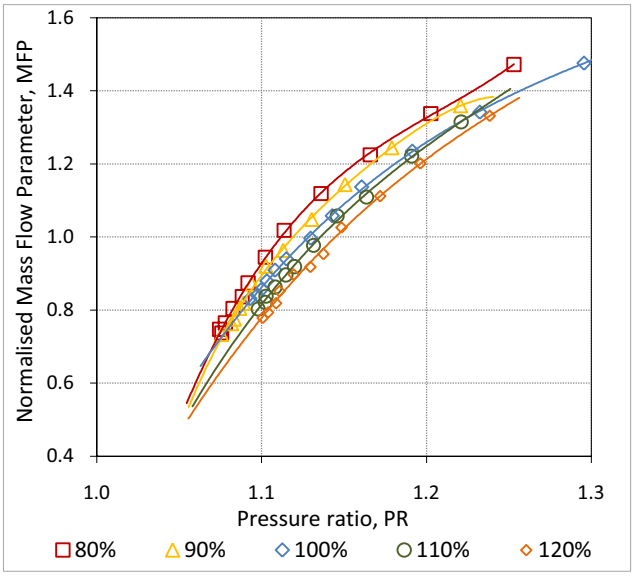

Figure 7: Normalised MFP vs. PR for cold-flow test

As for the turbine efficiency, the flow capacity of the low pressure turbine has been evaluated in terms of normalised Mass Flow Parameter, MFP and plotted versus the pressure ratio, PR as shown in Figure 7. From the figure it can be seen that the flow capacity of the low pressure turbine shows a typical trend common to all centrifugal machines; the MFP decreases as the rotational speed increases. A centrifugal pressure field opposed to the incoming mass flow is generated by the rotation of the turbine thus causing the drop of the flow capacity of the turbine as the speed increases [26]. As the pressure ratio increases the MFP reaches an asymptotic limit where further increases in pressure ratio will not result in any further increase in swallowing capacity (the turbine is choked). Despite within the current set of experiments the choking condition was not achieved, from the CFD analysis (which showed a good agreement with experimental results) it was found that the choking condition for the low pressure turbine is reached for pressure ratios greater than PR>1.4. Such a pressure ratio is well beyond the operating conditions of the low pressure turbine and therefore it will not be investigated any further.

1-D SIMULATION FOR ENGINE EFFECTIVENESS

The final goal for the low pressure turbine is that of assessing its influence on engine performance when installed in an engine as a part of the turbocompounding unit. At this purpose, a 1-D model for a turbocharged 1.0 litre 3 cylinders gasoline engine was developed and validated in an engine test bed; the turbocharger is externally waste-gated and the architecture of the baseline engine is shown in Figure 9. The baseline engine model was run for a range of constant engine speeds varying from 1,000 rpm to 6,000 rpm at steps of 500 rpm increase and the values of BSFC and BMEP were calculated. Then, the LPT was included in the engine model by using the performance maps obtained from the cold-flow testing in order to emulate the operating conditions of the turbocompounding. The model was run at similar operating conditions as the baseline engine and the additional power generated by the turbocompounding (≈ 1kW) was supplied directly to the crankshaft with the assumption of 100% mechanical efficiency. Three positions for the turbocompounding were investigated: (1) post-catalyst, (2) pre-catalyst and (3) in the waste gate (WG) of the main turbocharger (Figure 9). In order to meet the target of 1kW power output and 50,000 rpm of the rotational speed, an external wastegate had to be added to the LPT as shown in Figure 9.

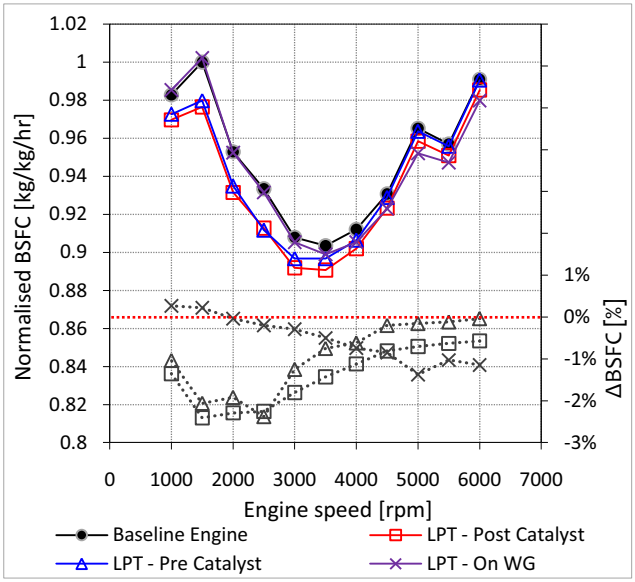

Figure 8: Impact of the LPT on BSFC

The outcomes of the simulation are reported in Figures 8 and 10 for which the normalised BSFC and BMEP for the three turbocompounding arrangements under study were plotted and compared to those obtained for the baseline engine[4]. In order to facilitate the discussion, in the secondary axis of both Figures 8 and 10 it was reported the percentage variation of both BSFC and BMEP with respect to the baseline engine model; the exact data are reported in Table 4 and Table 5 in greater details.

From Figure 8, it can be inferred that the addition of the turbocompounding unit is beneficial to the reduction of fuel consumption independently from its position in the engine. At low engine rpm (<2,000 rpm) the Pre and Post-catalyst position for the turbocompounding have a similar impact on BSFC with a

[4] The *BSFC* and the *BMEP* have been normalised to the maximum BSFC and BMEP values obtained for the baseline engine.

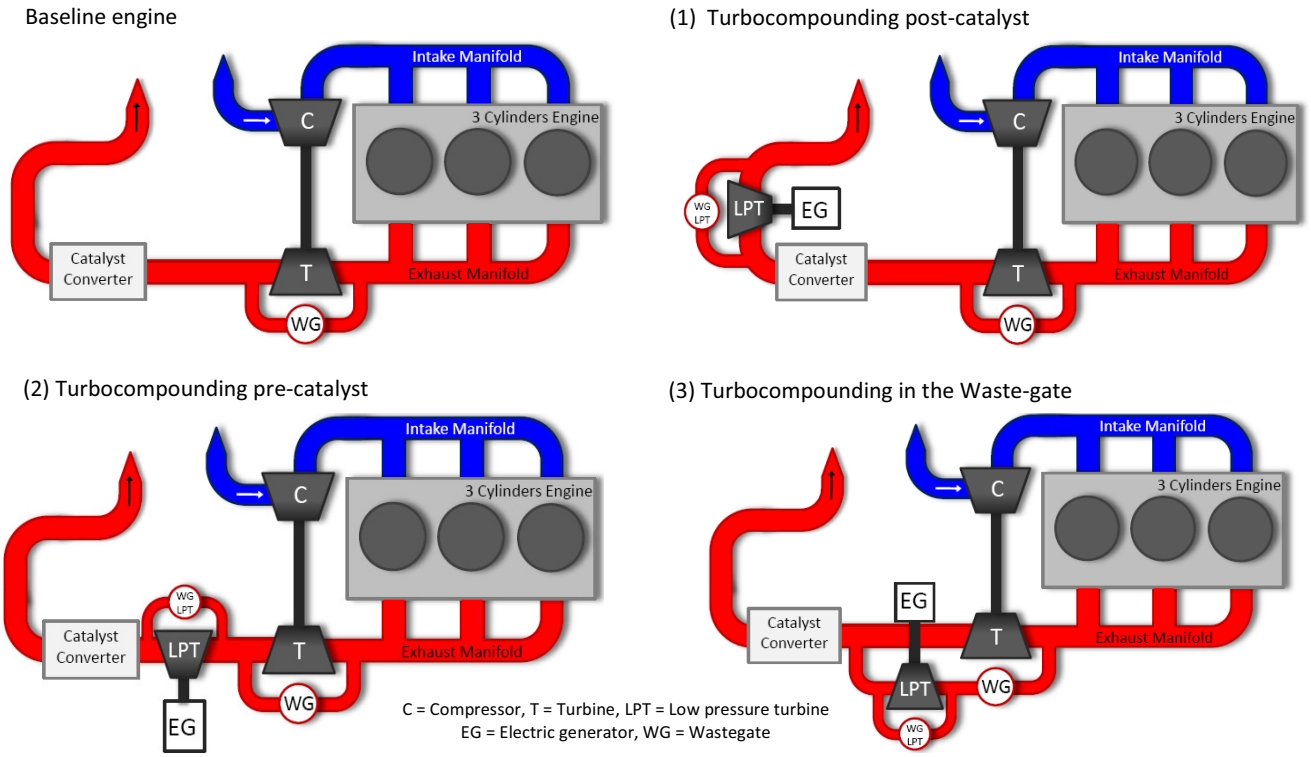

Figure 9: Positions of the low pressure turbine (LPT) as compared with the baseline engine

drop of more than 2% (max BSFC reduction was found for the Post-catalyst position at 1,500 engine rpm → ΔBSFC=-2.41%).

Nevertheless as the engine speed increases the benefits associated with the turcompounding deteriorate at a faster rate for the Pre-catalyst than the Post-catalyst position. For instance at 6,000 rpm the Pre-catalyst position offers in practice no reduction in fuel consumption (ΔBSFC = -0.04%) whereas the Post-catalyst still provides a 0.57% less fuel consumption. This can probably be attributed to higher amount of back-pressure due to the position of the turbocompounding which acts as a restrictor when it is located directly downstream of the main turbocharger (Pre-catalyst position).

This is further confirmed by the BSFC data obtained for the turbocompounding when positioned in the wastegate of the main turbocharger (= in parallel with the main turbocharger). Here it can be noticed that at high engine rpm the turbocompounding provides a reduction in BSFC twice as much (ΔBSFC ≈ -1%) that provided by the turbocompounding in the Pre and Post-catalyst position. This can be attributed to the fact that with such an arrangement the influence on back-pressure is minimised. Nevertheless the parallel position for the turbocompounding unit reveals to be inadequate to provide a significant reduction in BSFC at lower engine rpm. This can probably be attributed to the low power produced by the turbocompunding unit at low engine rpm (refer to Figure 12) as it will be explained later. Similarly to the BSFC the variation in BMEP showed some interesting features.

Figure 10 shows that the largest improvement in BMEP is obtained for the turbocompounding in the Post-catalyst position (ΔBMEP=2.21% at 1500 rpm) engine rpm (5500 rpm →6000 rpm) for which slightly negative values for the ΔBMEP were measured (-0.21% → -0.58%), the Post-catalyst solution has a positive impact on BMEP over the whole range of engine speeds. On the contrary the ΔBMEP obtained for the turbompounding in Pre-catalyst position is never as high as that obtained for the Post-catalyst position (apart for 1000 rpm) and the negative

Table 4: BSFC comparison for different LPT positions

Engine speed [rpm]	BSFC Pre Cat [kW/kg/hr]	ΔBSFC [%]	BSFC Post Cat [kW/kg/hr]	ΔBSFC [%]	BSFC On WG [kW/kg/hr]	ΔBSFC [%]
6000	0.991	-0.04%	0.991	-0.57%	0.980	-1.15%
5500	0.956	-0.12%	0.956	-0.63%	0.947	-1.03%
5000	0.964	-0.16%	0.964	-0.70%	0.952	-1.38%
4500	0.929	-0.20%	0.929	-0.81%	0.923	-0.85%
4000	0.906	-0.62%	0.906	-1.12%	0.905	-0.74%
3500	0.897	-0.75%	0.897	-1.43%	0.899	-0.50%
3000	0.897	-1.25%	0.897	-1.80%	0.905	-0.29%
2500	0.912	-2.38%	0.912	-2.26%	0.932	-0.20%
2000	0.935	-1.92%	0.935	-2.29%	0.952	-0.04%
1500	0.980	-2.06%	0.980	-2.41%	1.002	0.22%
1000	0.973	-1.04%	0.973	-1.35%	0.985	0.27%

Table 5: BMEP comparison for different LPT positions

Engine speed [rpm]	BMEP Pre Cat [kW/kg/hr]	ΔBMEP [%]	BMEP Post Cat [kW/kg/hr]	ΔBMEP [%]	BMEP On WG [kW/kg/hr]	ΔBMEP [%]
6000	0.802	-1.57%	0.810	-0.58%	0.819	0.57%
5500	0.886	-1.16%	0.895	-0.21%	0.902	0.67%
5000	0.947	-0.84%	0.956	0.15%	0.963	0.82%
4500	0.994	-0.61%	1.004	0.37%	1.008	0.79%
4000	0.992	-0.14%	1.001	0.75%	1.001	0.75%
3500	0.985	0.33%	0.993	1.13%	0.987	0.57%
3000	0.999	0.84%	1.006	1.48%	0.994	0.33%
2500	0.989	1.08%	0.999	2.01%	0.980	0.19%
2000	1.008	1.76%	1.012	2.17%	0.991	0.05%
1500	1.009	1.94%	1.012	2.21%	0.987	-0.24%
1000	0.677	3.86%	0.707	3.00%	0.649	-0.29%

impact on BMEP occurs at higher engine rpm, 4000 rpm → 6000 rpm, for which a ΔBMEP of -0.14% → -1.57% was measured. Finally BMEP was found to be almost insensitive to the turbocompounding when positioned in the main turbocharger wastegate. Again this can be considered to be as a direct consequence of the low power produced by the turbocompound unit when positioned in the wastegate, as shown in Figure 11.

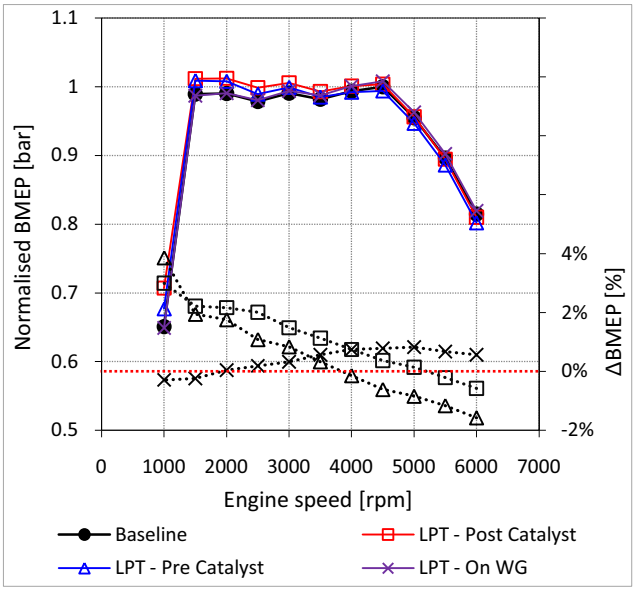

Figure 10: Impact of the LPT on BMEP

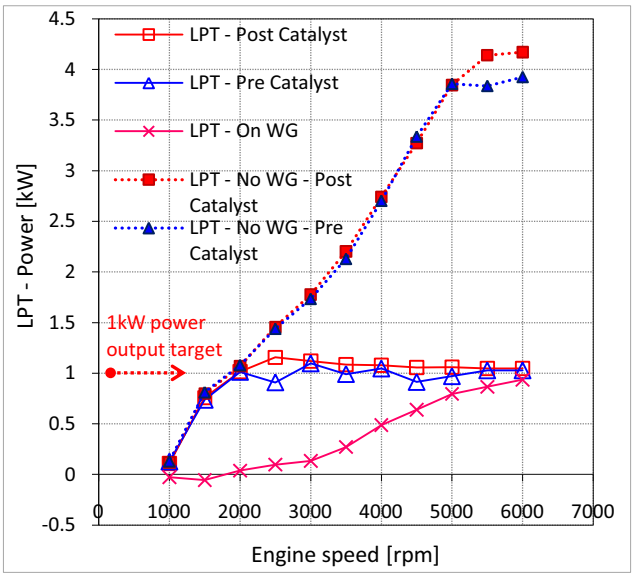

Figure 11: Power output for the LPT at 50000 rpm: comparison with the case where no constraint is set on max power.

Figure 11 reports the power generated by the tubocompound unit at constant rotational speed of 50,000 rpm. From the figure, it is apparent that the Pre and Post-catalyst arrangements succeed in providing the 1kW power target for almost any engine speed (apart for the 1500 engine rpm for which a power output of 0.73kW was calculated). The same does not occur for the turbocompounding installed in parallel with the main turbocharger. Figure 11 clearly shows that for such an arrangement, the power output from the turbocompound unit is always well below the 1kW target, in particular at low engine rpm for which even negative power was measured. This can be attributed to the fact that at low engine rpm the main turbocharger is only partly bypassed and so little mass flow is left to feed the turbocompond unit.

In addition to the analysis done on the power generated by the turbocompound unit under the constraints imposed by the requirements of the HyBoost project (refer to Table 1), an additional set of simulations was ran in order to assess the maximum power which could be generated by the turbocompound unit when no limitation on power output was set (but still maintaining the 50,000 rpm target). The outcomes are shown in Figure 11 where it can be noticed that with no constraint in power output, the actual power that could be generated by the turbocompound unit could go up to 4kW. This is quite interesting since it shows that the newly designed low pressure turbine could be applied to different sectors rather than small displacement engines. Further studies are currently being done in this direction and the outcomes will be subject of discussion in future publications.

CONCLUSIONS

This paper presented the outcomes of the design process of a high performance low pressure turbine for turbocompounding applications. The design requirements were set by the operating conditions of a 1.0 liter turbocharged gasoline engine with the low pressure turbine which had to operate at very low pressure ratios PR≈1.1 and generate 1kW at rotational speed of 50000 rpm.

The design process started with meanline modelling, followed by 2-D and CFD analysis which led to a turbine wheel of mixed-flow nature with very low value of inlet to exit area ratio (A_4/A_3 = 0.35). A prototype for the newly designed turbine was then produced and tested at the Imperial College cold-flow test facility. The turbine was tested for a range of constant speed lines spanning from 80% to 120% equivalent design speed. The experimental results showed that the newly designed turbine succeeds in achieving very high efficiencies ($\eta_{t\text{-}s}$ > 70%) for pressure ratios range (PR≈1.05-1.3) where conventional turbine usually provide less than 40%. This proves the effectiveness of the assumptions made during the design phase and it goes in favour of the use of the low pressure turbine in turbocompounding applications.

In order to assess the impact of the low pressure turbine on engine performance, a validated 1-D model of the 1.0 liter turbocharged gasoline engine under study was developed. Three different positions for the turbocompound unit (Pre-catalyst, Post-catalyst and in the wastegate of the main turbocharger) were analysed with respect to BSFC and BMEP and the outcomes were compared to those obtained from the baseline engine. The simulation results showed that the Post-catalyst position seems to provide the best compromise in terms of fuel consumption and engine performance with a max reduction in BSFC of 2.38% at 1500 rpm and a max improvement in BMEP of 2.4% at 1500rpm. The Pre-catalyst position exhibited similar BSFC values as those of the Post-catalyst position even though a deterioration of more than 1% was found for the BMEP (max BMEP variation was found at 6000 rpm → ΔBMEP=-1.57%). Finally the BSFC and BMEP calculated for the turbocompound unit when positioned in the wastegate of the main turbocharger were found to be insensitive to the presence of the turbocompound unit.

ACKNOWLEDGMENT

The authors would like to acknowledge Ricardo plc, CPT, Ford UK, Valeo, and Ealabc. This consortium along with Imperial College is part of the Hyboost project, a funded program by TSB (Technology strategy Board) whose support and encouragement is gratefully acknowledged.

The authors would also like to thank Universiti Teknologi MARA (UiTM) for its financial funding for the first author.

REFERENCES

[1] Taylor, A. M. K. P., "Science review of internal combustion engines," *Energy Policy*, Vol. 36, No. 12, 2008, pp. 4657-4667.

[2] Srinivasan, K. K., Mago, P. J., and Krishnan, S. R., "Analysis of exhaust waste heat recovery from a dual fuel low temperature combustion engine using an Organic Rankine Cycle," *Energy*, Vol. 35, No. 6, 2010, pp. 2387-2399.

[3] Zhelev, T. K. and Ridolfi, R., "Energy recovery and environmental concerns addressed through emergy-pinch analysis," *Energy*, Vol. 31, No. 13, 2006, pp. 2486-2498.

[4] Traverso, A., Magistri, L., and Massardo, A. F., "Turbomachinery for the air management and energy recovery in fuel cell gas turbine hybrid systems," *Energy*, Vol. 35, No. 2, 2010, pp. 764-777.

[5] Zmeureanu, R. and Yu Wu, X., "Energy and exergy performance of residential heating systems with separate mechanical ventilation," *Energy*, Vol. 32, No. 3, 2007, pp. 187-195.

[6] Zhao, F. Z. and Chang, S. Q., "Simulation and analysis of exhaust gas energy adjusting strategy in a hybrid turbocharged diesel engine," *Neiranji Xuebao/Transactions of CSICE (Chinese Society for Internal Combustion Engines)*, Vol. 26, No. 2, 2008, pp. 173-178.

[7] Franco, A. and Giannini, N., "A general method for the optimum design of heat recovery steam generators," *Energy*, Vol. 31, No. 15, 2006, pp. 3342-3361.

[8] Yamada, N., Minami, T., and Anuar Mohamad, M. N., "Fundamental experiment of pumpless Rankine-type cycle for low-temperature heat recovery," *Energy*, Vol. 36, No. 2, 2011, pp. 1010-1017.

[9] Fairbanks, J. W., "The 60 Percent Efficient Diesel Engine; Probable, Possible, or Just A Fantasy," *2005 Diesel Engine Emissions Reduction (DEER) Conference Presentations*, U.S Department of Energy, Chicago, Illinois, USA, 2005.

[10] Hopmann, U. and Algrain, M. C., "Diesel Engine Electric Turbo Compound Technology," *Future Transportation Technology Conference & Exhibition*, SAE International, Warrendale, USA, 2003.

[11] Kapich, D., "Turbo-Hydraulic Engine Exhaust Power Recovery System," *SAE Powertrain & Fluid Systems Conference & Exhibition*, San Diego, USA, 2002.

[12] Fraser, N., Blaxill, H., Lumsden, G., and Bassett, M., "Challenges for Increased Efficiency Through Gasoline Engine Downsizing," *SAE World Congress & Exhibition*, SAE International, New York, 2009.

[13] Thompson, I. G. M., Spence, S. W., McCartan, C. D., and Talbot-Weiss, J. M. H., "Design, validation, and performance result of a turbocharged turbogenerating biogas engine model," *9th International Conference on Turbochargers and Turbocharging*, Charlesworth Group, Wakerfeild, London, UK, 2010, pp. 11-22.

[14] Millo, F., Mallamo, F., Pautasso, E., and Mego, G. G., "The Potential of Electric Exhaust Gas Turbocharging for HD Diesel Engines," *SAE 2006 World Congress & Exhibition*, SAE International, Warrendale, USA, 2006.

[15] Karamanis, N., Palfreyman, D., Arcoumanis, C., and Martinez-Botas, R. F., "Steady and unsteady velocity measurements in a small turbocharger turbine with computational validation," *Journal of Physics: Conference Series*, Vol. 45, No. 1, 2006, pp. 1.

[16] Zhuge, W., Zhang, Y., Zheng, X., Yang, M., and He, Y., "Development of an advanced turbocharger simulation method for cycle simulation of turbocharged internal combustion engines," *Proceedings of the Institution of Mechanical Engineers, Part D: Journal of Automobile Engineering*, Vol. 223, No. 5, 2009, pp. 661-672.

[17] Abidat, M., Hachemi, M., Hamidou, M. K., and Baines, N. C., "Prediction of the steady and non-steady flow performance of a highly loaded mixed flow turbine," *Proceedings of the Institution of Mechanical Engineers, Part A: Journal of Power and Energy*, Vol. 212, No. 3 A3, 1998, pp. 173-184.

[18] Bin Mamat, A. M. I. and Martinez-Botas, R., "Mean Line Flow Model of Steady and Pulsating Flow Of a Mixed-Flow Turbine Turbocharger," *ASME TURBO Expo 2010: Power for Land, Sea and Air (GT2010)*, Glasgow, 2010.

[19] Palfreyman, D. and Martinez-Botas, R., "Numerical Study of the Internal Flow Filed Characteristics in Mixed Flow Turbines," *ASME TURBO EXPO 2002*, ASME, Amsterdam, Netherlands, 2002.

[20] Abidat, M., Chen, H., Baines, N. C., and Firth, M. R., "Design of a highly loaded mixed flow turbine," *Proceedings of the Institution of Mechanical Engineers, Part A: Journal of Power and Energy*, Vol. 206, No. 2, 1992, pp. 95-107.

[21] Rajoo, S. and Martinez-Botas, R., "Mixed flow turbine research: A review," *Journal of Turbomachinery*, Vol. 130, No. 4, 2008.

[22] Karamanis, N., Martinez-Botas, R. F., and Su, C. C., "Mixed flow turbines: Inlet and exit flow under steady and pulsating conditions," *Journal of Turbomachinery*, Vol. 123, No. 2, 2001, pp. 359-371.

[23] Palfreyman, D. and Martinez-Botas, R. F., "The pulsating flow field in a mixed flow turbocharger turbine: AN experimental and computational study," *2004 ASME Turbo Expo, June 14, 2004 - June 17, 2004*, Vol. 5 A, American Society of Mechanical Engineers, Vienna, Austria, 2004, pp. 697-708.

[24] Szymko, S.. The development of an eddy current dynamometer for evaluation of steady and pulsating turbocharger turbine performance. 2006. London, University of London; Imperial College.

[25] Szymko, S., McGlashan, N. R., Martinez-Botas, R., and Pullen, K. R., "The development of a dynamometer for torque measurement of automotive turbocharger turbines," *Proceedings of the Institution of Mechanical Engineers, Part D (Journal of Automobile Engineering)*, Vol. 221, No. D2, 2007, pp. 225-239.

[26] Arcoumanis, C., Hakeem, I., Khezzar, L., Martinez-Botas, R. F., and Baines, N. C., "Performance of a mixed flow turbocharger turbine under pulsating flow conditions," *Proceedings of the International Gas Turbine and Aeroengine Congress and Exposition, June 5, 1995 - June 8, 1995*, ASME, Houston, TX, USA, 1995, pp. 10pp.